


## Minimal-size real-space $d$ -wave pairing operator in $\text{CuO}_2$ planes

Adriana Moreo  and Elbio Dagotto

*Department of Physics and Astronomy, University of Tennessee, Knoxville, Tennessee 37966, USA  
and Materials Science and Technology Division, Oak Ridge National Laboratory, Oak Ridge, Tennessee 37831, USA*

 (Received 5 September 2019; revised manuscript received 21 October 2019; published 5 December 2019)

A novel minimal-size pairing operator  $\Delta_{D0}^\dagger$  with  $d$ -wave symmetry in  $\text{CuO}_2$  planes is introduced. This pairing operator creates on-site Cooper pairs at the four oxygens that surround a copper atom. Via the time evolution of  $\Delta_{D0}^\dagger$ , an additional interorbital pairing operator  $\Delta_{Dpd}^\dagger$  with  $d$ -wave symmetry is generated that pairs fermions located in a Cu and its four surrounding O atoms. The subsequent time evolution of  $\Delta_{Dpd}^\dagger$  generates an intraorbital  $d$ -wave pairing operator  $\Delta_{Dpp}^\dagger$  involving the four O atoms that surround a Cu atom, as well as the  $d$ -wave operator  $\Delta_D^\dagger$  traditionally used in single-band models for cuprates. Because we recover the larger size operators extensively used in the three-orbital Hubbard model, we suggest that long-range order using the canonical extended operators occurs together with long-range order in the new minimal operators. However, our minimal  $d$ -wave operators could be more practical to study  $d$ -wave superconductivity because in the finite-size relatively small systems accessible to computational techniques it is easier to observe long-range order using local operators. Moreover, an effective model with the usual tight-binding hopping of the  $\text{CuO}_2$  planes supplemented by an attractive potential  $V$  in the  $d$ -wave channel is introduced. Using mean-field techniques, we show that a paired ground state is stabilized for any finite value of  $V$ . We observed that the values of  $V$  that lead to gap sizes similar to those in the cuprates are smaller for  $d$ -wave pairing operators that include Cu  $d$  orbitals than those that include only  $p$  orbitals. In all cases the gap that opens in the spectrum has standard  $d$ -wave symmetry. Finally, a simpler effective model is introduced to study the phenomenology of multiorbital  $d$ -wave superconductors, similar to how the negative- $U$  Hubbard model is used for properties of  $s$ -wave superconductors.

DOI: [10.1103/PhysRevB.100.214502](https://doi.org/10.1103/PhysRevB.100.214502)

### I. INTRODUCTION

The discovery of  $d$ -wave superconductivity in the high-critical-temperature cuprates [1,2] started efforts to develop effective Hamiltonians that would allow us to study  $d$ -wave pairing in the same way as the negative- $U$  Hubbard model allows the study of  $s$ -wave pairing in standard BCS superconductors [3–5]. Previous efforts focused on single-orbital systems with on-site Coulomb repulsion together with an effective attractive nearest-neighbor potential [6,7] or hardcore dimers [8] or via the phenomenological addition of a term proportional to the square of the nearest-neighbor hoppings [9]. These models were difficult to study, parameters needed to be fine-tuned, and actual numerical evidence of long-range  $d$ -wave pairing correlations has been elusive [10]. The contribution of orbital degrees of freedom to the symmetry of the pairing operator came to the foreground when superconductivity was observed in iron-based pnictides and selenides [11–14], and recently, an effective model with on-site interorbital attraction was presented [15]. While relatively easy to study, interorbital same-site pairing operators are considered to be less likely to develop long-range order than their intraorbital counterparts involving the same orbital but at different sites. For all these reasons, it is still important to find alternative and practical intraorbital pairing operators with  $d$ -wave symmetry.

In addition, recent angle-resolved photoemission experiments using  $\text{Bi}_2\text{Sr}_2\text{CaCu}_2\text{O}_{8+\delta}$  indicated a novel “starfish”

shape of the superconducting pairs with a very short length—of the order of one lattice space—in the antinodal direction [16]. This unexpected result appears to be doping independent, and it may offer clues on the local structure of  $d$ -wave pairs in the strong-coupling regime. For us these experiments provide additional motivation to reconsider the local form of the  $d$ -wave pairing operators in the cuprates.

Most previous attempts to construct same-orbital effective  $d$ -wave models, analogous to the  $U < 0$  Hubbard model for  $d$ -wave, relied on single-orbital systems with electrons placed on sites of a square lattice that mimic only the coppers. In the present paper, we aim to explore whether effective models for  $d$ -wave superconductivity can be constructed using, instead, the oxygen locations in the more realistic  $\text{CuO}_2$  lattice. It is well known that holes tend to reside on oxygens due to the charge transfer nature of the cuprates. However, the vast majority of theory efforts in this context rely on one-orbital Cu-only models, such as the  $t$ - $J$  and one-orbital Hubbard. Only recently have computational efforts to study the full  $\text{CuO}_2$  models, with both Cu and O incorporated, been carried out, and interesting results such as stripes have already been unveiled in this context [17–19]. Thus, our focus and main question addressed are timely: can we find an effective model for  $d$ -wave superconductivity using only the oxygens of a  $\text{CuO}_2$  lattice, namely, only the atoms placed at the bonds of said square lattice? Moreover, in searching for the most compact form for this pairing operator we will address, as a bonus, the recent photoemission results in the cuprates that unveiled

very small Cooper pairs, at least in the antinodal directions [16]. Our overarching goal can be framed similarly to early studies within one-orbital models that attempted to construct quasiparticle operators with a larger quasiparticle weight  $Z$  than those of the usual bare operators (i.e., better “antennas”) and thus derive pairing operators that could produce stronger signals in computational studies [20].

This paper is organized as follows: in Sec. II the models traditionally used to study the cuprates, as well as the  $d$ -wave pairing operators previously investigated, are discussed. Our new minimal  $d$ -wave pairing operator in the CuO<sub>2</sub> planes is introduced in Sec. III, while in Sec. IV additional  $d$ -wave pairing operators, including the more standard extended ones, are deduced by calculating the time evolution of the minimal operator. Both the minimal and some extended pairing operators are studied at the mean-field level in Sec. V, and a simple effective model is introduced in Sec. VI. Section VII is devoted to our conclusions.

## II. MODELS AND PREVIOUSLY USED $d$ -WAVE PAIRING OPERATORS FOR CUPRATES

It is widely accepted that a realistic model to describe CuO<sub>2</sub> planes is a three-orbital Hubbard model that includes the  $d_{x^2-y^2}$  orbitals at the coppers and the  $p_\sigma$  orbitals at the oxygens at a distance  $\hat{\mu}/2$  from the coppers (lattice constant units), with  $\hat{\mu} = x$  or  $y$  [21], i.e., along the two directions. The Hamiltonian is

$$H_{3\text{BH}} = H_{\text{TB}} + H_{\text{int}}, \quad (1)$$

where

$$\begin{aligned} H_{\text{TB}} = & -t_{pd} \sum_{\mathbf{i}, \mu, \sigma} \alpha_{\mathbf{i}, \mu} (p_{\mathbf{i}+\frac{\hat{\mu}}{2}, \mu, \sigma}^\dagger d_{\mathbf{i}, \sigma} + \text{H.c.}) \\ & - t_{pp} \sum_{\mathbf{i}, \langle \mu, \nu \rangle, \sigma} \alpha'_{\mathbf{i}, \mu, \nu} [p_{\mathbf{i}+\frac{\hat{\mu}}{2}, \mu, \sigma}^\dagger (p_{\mathbf{i}+\frac{\hat{\nu}}{2}, \nu, \sigma} + p_{\mathbf{i}-\frac{\hat{\nu}}{2}, \nu, \sigma}) \\ & + \text{H.c.}] \\ & + \epsilon_d \sum_{\mathbf{i}} n_{\mathbf{i}}^d + \epsilon_p \sum_{\mathbf{i}, \mu} n_{\mathbf{i}+\frac{\hat{\mu}}{2}}^p + \mu_e \sum_{\mathbf{i}, \mu} (n_{\mathbf{i}+\frac{\hat{\mu}}{2}}^p + n_{\mathbf{i}}^d) \end{aligned} \quad (2)$$

and

$$H_{\text{int}} = U_d \sum_{\mathbf{i}} n_{\mathbf{i}, \uparrow}^d n_{\mathbf{i}, \downarrow}^d + U_p \sum_{\mathbf{i}, \mu, \sigma} n_{\mathbf{i}+\frac{\hat{\mu}}{2}, \uparrow}^p n_{\mathbf{i}+\frac{\hat{\mu}}{2}, \downarrow}^p. \quad (3)$$

The operator  $d_{\mathbf{i}, \sigma}^\dagger$  creates an electron with spin  $\sigma$  at site  $\mathbf{i}$  of the copper square lattice, while  $p_{\mathbf{i}+\frac{\hat{\mu}}{2}, \mu, \sigma}^\dagger$  creates an electron with spin  $\sigma$  at orbital  $p_\mu$ , where  $\mu = x$  or  $y$ , for the oxygen located at  $\mathbf{i} + \frac{\hat{\mu}}{2}$ . The hopping amplitudes  $t_{pd}$  and  $t_{pp}$  correspond to the hybridizations between nearest-neighbor Cu-O and O-O, respectively, and  $\langle \mu, \nu \rangle$  indicate O-O pairs connected by  $t_{pp}$ , as shown in Fig. 1.  $n_{\mathbf{i}+\frac{\hat{\mu}}{2}, \sigma}^p$  ( $n_{\mathbf{i}, \sigma}^d$ ) is the number operator for  $p$  ( $d$ ) electrons with spin  $\sigma$ , and  $\epsilon_d$  and  $\epsilon_p$  are the on-site energies at the Cu and O sites, respectively. The Coulomb repulsion between two electrons at the same site and orbital is  $U_d$  ( $U_p$ ) for  $d$  ( $p$ ) orbitals. The signs of the Cu-O and O-O hoppings due to the symmetries of the orbitals is included in the parameters  $\alpha_{\mathbf{i}, \mu}$  and  $\alpha'_{\mathbf{i}, \mu, \nu}$  and follow the convention shown in Fig. 1. Finally,  $\mu_e$  is the electron chemical potential.

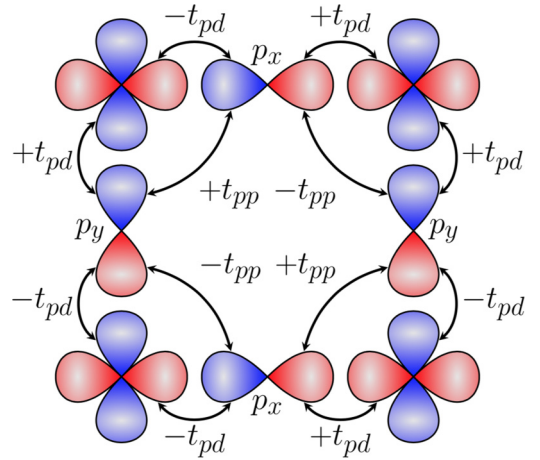


FIG. 1. Schematic drawing of the Cu  $d_{x^2-y^2}$  orbitals at the copper sites of the square lattice, with the sign convention indicated by the colors (red for + and blue for -). The oxygen  $p_\sigma$  orbitals with their corresponding sign convention are also shown, located at the Cu-O-Cu bonds. The sign convention for the  $t_{pd}$  and  $t_{pp}$  hoppings is also presented.

The hopping parameters are those much used for the cuprates, i.e.,  $t_{pd} = 1.3$  eV and  $t_{pp} = 0.65$  eV; on-site energy  $\epsilon_p = -3.6$  eV [22], and  $\Delta_{CT} = \epsilon_d - \epsilon_p$ , which is positive ( $\epsilon_d = 0$ ) [23], is the charge-transfer gap.

### A. Single-orbital $d$ -wave operators

Because experiments indicate that the Fermi surface of the cuprates is determined by a single band [24–27] and, theoretically, a mapping of the three-band Hubbard model to the  $t$ - $J$  Hamiltonian can be obtained via Zhang-Rice singlets [28], using only one band is appealing. In fact, due to their relative simplicity, the study of single-orbital models has prevailed in the cuprates. As a result, the simplest pairing operators with  $d$ -wave symmetry are extended in the sense that they involve nearest-neighbor Cu sites [29,30], without the oxygens in between. Zhang and Rice studied the addition of one hole in an undoped three-orbital Hubbard model using a CuO<sub>4</sub> cluster but neglecting the O-O hopping. They found that the hole occupies a symmetric linear combination involving the four O atoms around a Cu and forms a spin singlet together with the hole in the central Cu [28]. They also showed that the energy of the small cluster with two extra holes in the O orbitals was higher than the energy of two separated O holes. The next step was to construct Wannier functions combining the single-cluster symmetric single-hole plaquette states and obtain the effective single-orbital low-energy model, leading to the  $t$ - $J$  model. As discussed earlier, the simplest  $d$ -wave pairing operator in the  $t$ - $J$  (and one-orbital Hubbard) modes involves nearest-neighbor sites and has the well-known form

$$\Delta_D^\dagger(\mathbf{j}) = \sum_{\mu, \sigma} f(\sigma) \gamma_\mu c_{\mathbf{j}+\hat{\mu}, \sigma}^\dagger c_{\mathbf{j}, -\sigma}^\dagger, \quad (4)$$

where  $c_{\mathbf{j}, \sigma}^\dagger$  creates an electron with spin  $\sigma$  at site  $\mathbf{j}$  of the Cu square lattice [see Fig. 2(a)],  $\gamma_\mu = 1$  ( $-1$ ) for  $\mu = \pm x$  ( $\pm y$ ) and  $f(\sigma) = 1$  ( $-1$ ) if  $\sigma = \uparrow$  ( $\downarrow$ ).

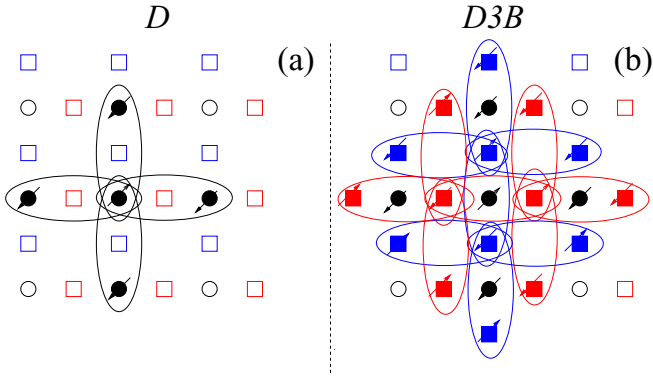


FIG. 2. Schematic drawing of previously used  $d$ -wave pairing operators in the  $\text{CuO}_2$  planes. Circles indicate the Cu  $d$ -orbital sites, while red (blue) squares indicate the O  $p_x$  ( $p_y$ ) orbital sites. Solid symbols indicate atoms where the particles forming the Cooper pairs are located, and arrows indicate the spin of the electrons and holes in the pair. (a) In single-orbital approximations to the  $\text{CuO}_2$  planes the Cooper pairs are assumed to be primarily located in nearest-neighbor Cu sites via the operator  $\Delta_D^\dagger$ . (b) In the three-orbital Hubbard model the  $d$ -wave pairing operator  $\Delta_{D3B}^\dagger$  adds Cooper pairs involving  $p_x$  and  $p_y$  orbitals, in addition to the Cu orbitals as in (a) not shown in this panel for clarity. The individual Cooper pairs are encircled with ellipses. The relative phases are positive along  $x$  and negative along  $y$ .

### B. Three-orbital extended $d$ -wave operators

Note that the empty sites (holes) in the effective  $t$ - $J$  model contain Zhang-Rice singlets (ZRSs), which means that the components of the Cooper pair in Eq. (4) are created on top of the ZRSs. The first numerical calculations studying pairing were performed in single-orbital models [29], and when, later on, pairing was numerically evaluated in three-orbital Hubbard models, the pairing operators used [18,31,32] were straightforward generalizations of Eq. (4) [see Fig. 2(b)] involving several sites, such as

$$\begin{aligned} \Delta_{D3B}^\dagger(\mathbf{j}) = & \sum_{\mu,\sigma} f(\sigma) \gamma_\mu [d_{\mathbf{j}+\hat{\mu},\sigma}^\dagger d_{\mathbf{j},-\sigma}^\dagger \\ & + P_{\mathbf{j}+\hat{\mu}+x/2,x,\sigma}^\dagger P_{\mathbf{j}+x/2,x,-\sigma}^\dagger \\ & + P_{\mathbf{j}+\hat{\mu}+y/2,y,\sigma}^\dagger P_{\mathbf{j}+y/2,y,-\sigma}^\dagger]. \end{aligned} \quad (5)$$

This operator creates electrons that form intraorbital pairs whose  $d$ -wave symmetry is determined by  $\gamma_\mu$ . It considers that Cooper pairs are formed by one electron (or hole) in a Cu and another in its neighboring Cu atoms, with a similar consideration for electrons (or holes) in the  $p$  orbitals. It is in this sense that this operator is intraorbital: the pair terms involve either Cu or O. In real space the minimum pair created by the pairing operators in Eqs. (4) and (5) involves five lattice sites in a single-orbital model context or several unit cells (21 Cu and O sites) for the three-orbital case. Such extended pairing operators [see Figs. 2(a) and 2(b)] appear to be at odds with the recent experimental results of Ref. [16], where the observed pairs have a minimum real-space extension of the order of the lattice constant along the antinodal direction. This photoemission experiment offers motivation to investigate whether in the  $\text{CuO}_2$  planes it is possible to construct a more

local  $d$ -wave pairing operator involving far fewer sites and ideally just one unit cell.

### III. MINIMAL $d$ -WAVE PAIRING OPERATOR

As explained, in undoped systems and in the Zhang-Rice approximation a doped hole is placed at an oxygen and forms a ZRS with the hole at a copper. A second doped hole is expected to form another ZRS with a different Cu. The one-orbital pairing operator in Eq. (4) can involve only electrons at two neighboring Cu sites, each with its own ZRS. However, in the three-orbital Hubbard model formulation there is no clear relation between the pairing operator and the two neighboring ZRSs. Equation (5) just considers that the minimal Cooper pair can be formed by fermions at a  $d$  ( $p_\sigma$ ) orbital and at the four nearest-neighbor Cu (O) atoms, thus involving five unit cells and many sites.

As discussed above, Zhang and Rice found out that it would be unlikely that two holes would share the O orbitals of one single plaquette. However, calculations including  $t_{pp}$  hopping and the  $p$ - $d$  Coulomb repulsion, both neglected in the ZRS derivation, indicated that an effective attraction between holes in the oxygens of a single plaquette may develop [33,34]. Thus, the possibility that two holes could form a pair in the O orbitals in a single plaquette deserves to be explored.

First, we will construct an on-site  $d$ -wave pairing operator which considers only *doubly occupied* O sites [see Fig. 3(a)], in analogy with the on-site attractive  $s$ -wave pairing operator. It has the form

$$\begin{aligned} \Delta_{D0}^\dagger(\mathbf{j}) = & \frac{1}{2} \sum_{\mu,\sigma} f(\sigma) \gamma_\mu P_{\mathbf{j}+\hat{\mu}/2,\mu,\sigma}^\dagger P_{\mathbf{j}+\hat{\mu}/2,\mu,-\sigma}^\dagger \\ = & \sum_{\mu} \gamma_\mu P_{\mathbf{j}+\hat{\mu}/2,\mu,\uparrow}^\dagger P_{\mathbf{j}+\hat{\mu}/2,\mu,\downarrow}^\dagger. \end{aligned} \quad (6)$$

Although the operator involves doubly occupied sites, each one apparently  $s$  wave, since the operator involves four oxygens around the same copper, a linear combination can be made that renders the full operator  $d$ -wave.

### IV. TIME-EVOLUTION OF THE PAIRING OPERATOR

In previous literature [35,36] a relationship between the on-site and the extended  $s$ -wave pairing operators in the single-orbital Hubbard model was obtained by calculating the time evolution of the on-site pairing operator. Following similar steps, we can now calculate the time evolution of the on-site minimal  $d$ -wave pairing operator  $\Delta_{D0}^\dagger$  proposed in Eq. (6) for the three-orbital Hubbard model Eq. (1). We found that

$$\begin{aligned} -i \frac{d\Delta_{D0}^\dagger}{dt} = & [H_{3BH}, \Delta_{D0}^\dagger] \\ = & 2(\epsilon_p - \mu_e) \Delta_{D0}^\dagger - U_p \Delta_{D0}^\dagger - t_{pd} \Delta_{Dpd}^\dagger, \end{aligned} \quad (7)$$

where  $\Delta_{Dpd}^\dagger$  is another  $d$ -wave pairing operator defined in one unit-cell  $\text{CuO}_2$ .  $\Delta_{Dpd}^\dagger$  forms Cooper pairs with one fermion at a Cu and the other in an antisymmetric linear combination of the  $p_\sigma$  orbitals in its four nearest-neighbor O atoms [Fig. 3(c)],

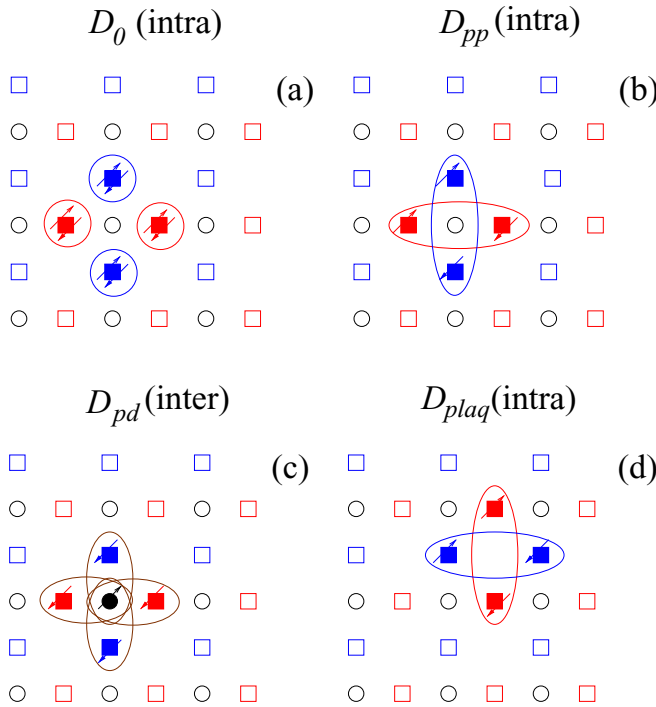


FIG. 3. Schematic drawing of the minimal intraunit cell  $d$ -wave pairing operators for the  $\text{CuO}_2$  planes that were not explored before in three-orbital Hubbard models to our knowledge. Circles indicate the Cu  $d$  orbitals, while the red (blue) squares indicate the  $p_x$  ( $p_y$ ) orbitals at the O atoms. Solid symbols indicate sites where the particles forming the Cooper pairs are located, and arrows indicate the spin of the electrons and holes in the pair. (a) On-site intraorbital (i.e., same oxygen)  $d$ -wave operator  $\Delta_{D_0}^\dagger$ , defined in Eq. (6). Here the two members of the Cooper pair are at the same oxygen, linearly combined, involving the four possible oxygens. (b) More extended nearest-neighbor intraorbital  $d$ -wave operator  $\Delta_{D_{pp}}^\dagger$  where the Cooper pair is formed by two electrons in the same  $p_\sigma$  orbital, either  $x$  or  $y$ , at a distance of one lattice spacing, forming a spin singlet and linearly combining the vertical and horizontal directions to form a  $d$ -wave operator. (c) Interorbital ( $dp$ )  $d$ -wave operator  $\Delta_{D_{pd}}^\dagger$  with pairs involving a particle at the central Cu and the other at a neighboring O, linearly combined to form a  $d$ -wave. (d) Plaquette  $d$ -wave intraorbital pairing operator  $\Delta_{D_{plaq}}^\dagger$  in the  $\text{CuO}_2$  plane. In (a)–(d), the Cooper pairs are encircled with ellipses. Relative phases are positive along  $x$  and negative along  $y$ , leading to a  $d$ -wave.

and it is given by

$$\Delta_{D_{pd}}^\dagger(\mathbf{j}) = \sum_{\mu,\sigma} f_\sigma \gamma_\mu \alpha_{\mathbf{j},\mu} d_{\mathbf{j},\sigma}^\dagger p_{\mathbf{j}+\hat{\mu}/2,\mu,-\sigma}^\dagger. \quad (8)$$

Since in the ground state the average value of the pairing operators is time independent, from Eq. (7) we see that the average values of the two pairing operators must be related. In addition, by evaluating the time evolution of the new interorbital minimal pairing operator  $\Delta_{D_{pd}}^\dagger$ , more extended intra- and interorbital pairing operators with  $d$ -wave symmetry are obtained. For example, from the commutator between  $\Delta_{D_{pd}}^\dagger$  and  $H_{pd}$ , the  $t_{pd}$  hopping term in  $H_{3\text{BH}}$  [37], we obtain the nearest-neighbor  $d$ -orbital pairing operator in Eq. (4) depicted in Fig. 2(a) and an additional intraorbital pairing operator

given by

$$\begin{aligned} \Delta_{D_{pp}}^\dagger(\mathbf{j}) &= (p_{\mathbf{j}+x/2,x,\uparrow}^\dagger p_{\mathbf{j}-x/2,x,\downarrow}^\dagger - p_{\mathbf{j}+x/2,x,\downarrow}^\dagger p_{\mathbf{j}-x/2,x,\uparrow}^\dagger) \\ &\quad - (p_{\mathbf{j}+y/2,y,\uparrow}^\dagger p_{\mathbf{j}-y/2,y,\downarrow}^\dagger - p_{\mathbf{j}+y/2,y,\downarrow}^\dagger p_{\mathbf{j}-y/2,y,\uparrow}^\dagger) \\ &= \sum_{\mu,\sigma} f_\sigma \gamma_\mu p_{\mathbf{j}+\hat{\mu}/2,\mu,\sigma}^\dagger p_{\mathbf{j}-\hat{\mu}/2,\mu,-\sigma}^\dagger, \end{aligned} \quad (9)$$

which is another  $B_{1g}$  intraorbital pairing operator with the two particles located in the same orbital but at different oxygens [see Fig. 3(b)] and it is analogous to the extended, nearest-neighbor,  $s$ -wave operator defined in the context of the cuprates [29,35]. In addition, the commutator between  $\Delta_{D_{pp}}^\dagger$  and  $H_{pp}$ , the  $t_{pp}$  hopping term in  $H_{3\text{BH}}$ , leads to an extended version of  $\Delta_{D_{pp}}^\dagger$  that forms pairs with one fermion on a  $d$  orbital at site  $\mathbf{r}$  and the other at orbital  $p_x$  ( $p_y$ ) at distance  $\mathbf{r} + \mathbf{y} + x/2$  ( $\mathbf{r} + x + y/2$ ) and symmetrical points [38]. The commutator of this extended operator with the  $t_{pd}$  hopping term in  $H_{3\text{BH}}$  finally leads to  $p$ -orbital pairing operators that combine fermions in  $p_x$  ( $p_y$ ) orbitals along the  $y$  ( $x$ ) direction which are the plaquette pairing operators mentioned in Ref. [16] and shown in Fig. 3(d). They are given by

$$\begin{aligned} \Delta_{D_{plaq}}^\dagger(\mathbf{j}) &= (p_{\mathbf{j}+x/2,x,\uparrow}^\dagger p_{\mathbf{j}+y+x/2,x,\downarrow}^\dagger \\ &\quad - p_{\mathbf{j}+x/2,x,\downarrow}^\dagger p_{\mathbf{j}+y+x/2,x,\uparrow}^\dagger) \\ &\quad - (p_{\mathbf{j}+y/2,y,\uparrow}^\dagger p_{\mathbf{j}+x+y/2,y,\downarrow}^\dagger \\ &\quad - p_{\mathbf{j}+y/2,y,\downarrow}^\dagger p_{\mathbf{j}+x+y/2,y,\uparrow}^\dagger) \\ &= \sum_{\mu,\sigma} f_\sigma \gamma_\mu p_{\mathbf{j}+\hat{\mu}/2,\mu,\sigma}^\dagger p_{\mathbf{j}+\hat{\mu}+\hat{\mu}/2,\mu,-\sigma}^\dagger, \end{aligned} \quad (10)$$

where  $\hat{\mu} = x$  ( $y$ ) if  $\mu = y$  ( $x$ ). We also notice that the  $p$  contribution in the standard  $d$ -wave pairing operator in Eq. (5) results from a combination of the intraorbital  $p$  pairing operators  $\Delta_{D_{plaq}}^\dagger$  and  $\Delta_{D_{pp}}^\dagger$ .

The relationships between the minimal and compact, but more extended,  $d$ -wave pairing operators in Fig. 3 deduced from the time-evolution calculations suggest that if the Hamiltonian indeed has a superconducting ground state with  $d$ -wave symmetry, we would expect that *all* the pairing operators with that symmetry will develop long-range order simultaneously. In practice we expect the long-range behavior of local operators to be easier to study in the finite, often small, clusters accessible to numerical studies. For this reason, we will focus on the  $d$ -wave pairing operators introduced in Fig. 3, and we will compare them with the traditional ones presented in Fig. 2.

## V. EFFECTIVE MODEL FOR $d$ -WAVE PAIRING

To show explicitly that the pairing operators in Eqs. (6), (8), (9), and (10) indeed lead to  $d$ -wave superconductors we will study the phenomenological Hamiltonian given by

$$H_{3\text{BDW}} = H_{\text{TB}} + H_{\text{int}}, \quad (11)$$

where the tight-binding term is the canonical of the three-orbital Hubbard model for cuprates [Eq. (2)] and the interacting portion of the Hamiltonian for the on-site same-oxygen

pairing, as in  $D_0$ , is given by

$$H_{\text{int}}^{(0)} = - \sum_{\mathbf{j}, \mu, \sigma} \gamma_{\mu} f(\sigma) [p_{\mathbf{j}+\hat{\mu}/2, \mu, \sigma}^{\dagger} p_{\mathbf{j}+\hat{\mu}/2, \mu, -\sigma}^{\dagger} \Delta + \Delta^* p_{\mathbf{j}-\hat{\mu}/2, \mu, -\sigma} p_{\mathbf{j}-\hat{\mu}/2, \mu, \sigma}]. \quad (12)$$

$\Delta$  and  $\Delta^*$  are parameters that determine the strength of the superconducting condensate, and they also contain the attractive coupling  $V$  usually employed in these phenomenological models. For the case of the interorbital extended pairing  $\Delta_{Dpd}^{\dagger}$  the interaction term is given by

$$H_{\text{int}}^{(pd)} = - \sum_{\mathbf{j}, \mu, \sigma} \gamma_{\mu} f(\sigma) \alpha_{\mathbf{j}, \mu} [d_{\mathbf{j}, \sigma}^{\dagger} p_{\mathbf{j}-\mu/2, \mu, -\sigma}^{\dagger} \Delta + \Delta^* p_{\mathbf{j}-\mu/2, \mu, -\sigma} d_{\mathbf{j}, \sigma}]. \quad (13)$$

For the intraorbital extended pairing  $\Delta_{Dpp}^{\dagger}$  the interaction term is given by

$$H_{\text{int}}^{(pp)} = - \sum_{\mathbf{j}, \mu, \sigma} \gamma_{\mu} f(\sigma) [p_{\mathbf{j}+\hat{\mu}/2, \mu, \sigma}^{\dagger} p_{\mathbf{j}+\hat{\mu}/2, \mu, -\sigma}^{\dagger} \Delta + \Delta^* p_{\mathbf{j}-\hat{\mu}/2, \mu, -\sigma} p_{\mathbf{j}+\hat{\mu}/2, \mu, \sigma}], \quad (14)$$

while for the plaquette operator  $\Delta_{Dplaq}^{\dagger}$  the interaction is given by

$$H_{\text{int}}^{(plaq)} = - \sum_{\mathbf{j}, \mu, \sigma} \gamma_{\mu} f(\sigma) [p_{\mathbf{j}+\hat{\mu}/2, \bar{\mu}, \sigma}^{\dagger} p_{\mathbf{j}-\hat{\mu}/2, \bar{\mu}, -\sigma}^{\dagger} \Delta + \Delta^* p_{\mathbf{j}-\hat{\mu}/2, \bar{\mu}, -\sigma} p_{\mathbf{j}+\hat{\mu}/2, \bar{\mu}, \sigma}]. \quad (15)$$

### A. Mean-field analysis

In this section we perform a canonical mean-field analysis of the effective pairing models now using our more compact  $d$ -wave operators. As usual, via a Fourier transform we can work in momentum space, which is more convenient. Thus,  $H_{\text{TB}}$  can be written as

$$H_{\text{TB}}(\mathbf{k}) = \sum_{\mathbf{k}, \sigma} \Phi_{\mathbf{k}, \sigma}^{\dagger} \xi_{\mathbf{k}} \Phi_{\mathbf{k}, \sigma}, \quad (16)$$

where  $\Phi_{\mathbf{k}, \sigma}^{\dagger} = (p_x^{\dagger}(\mathbf{k}), p_y^{\dagger}(\mathbf{k}), d^{\dagger}(\mathbf{k}))_{\sigma}$  and

$$\xi_{\mathbf{k}} = \begin{pmatrix} \epsilon_p & -4t_{pp}s_x s_y & -2it_{pd}s_x \\ -4t_{pp}s_x s_y & \epsilon_p & -2it_{pd}s_y \\ 2it_{pd}s_x & 2it_{pd}s_y & 0 \end{pmatrix}, \quad (17)$$

where  $s_i$  indicates  $\sin(k_i/2)$ , with  $i = x$  or  $y$ .

Note that in the electron representation the undoped case is characterized by one hole at the Cu and no holes at the O, which corresponds to a total of five electrons per  $\text{CuO}_2$  unit cell (the maximum possible electronic number in three orbitals is six). The orbital-resolved tight-binding bands along the  $\Gamma$ - $X$ - $M$ - $\Gamma$  path in the Brillouin zone calculated using a  $100 \times 100$  square lattice (with Cu atoms at the sites of the lattice) is shown in Fig. 4. The dashed black line is the chemical potential  $\mu_e$  for the important electronic density  $\langle n \rangle = 5$ , and the corresponding Fermi surface is given in the inset. An analysis of the orbital composition of each of the three bands, shown by the color palette, indicates that the top band is purely  $d$  at the  $\Gamma$  point and, moving away from  $\Gamma$ , becomes hybridized with the  $p$  orbitals such that its  $d$  content

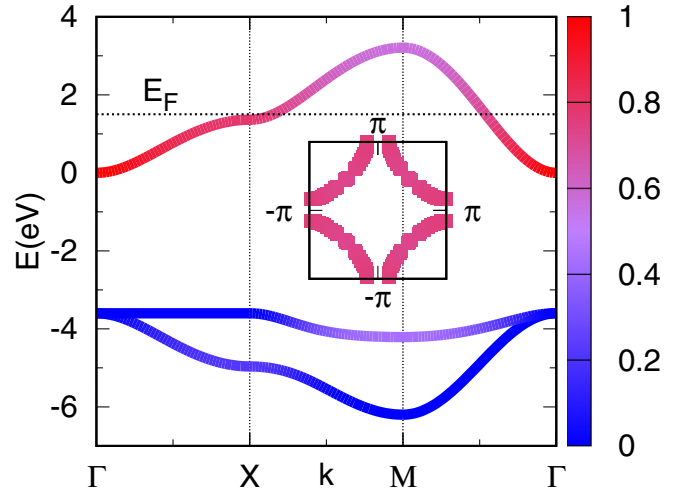


FIG. 4. Band dispersion for the tight-binding term of the  $\text{CuO}_2$  Hamiltonian. The orbital content is displayed with red (blue) indicating  $d$  ( $p$ ) character. The dashed line indicates the position of the chemical potential (or Fermi level  $E_F$ ) at density  $\langle n \rangle = 5$  (undoped case). The Fermi surface at this density is in the inset. Colors indicate the orbital content of the bands, with the palette on the right denoting the weight of the  $d$  component (e.g., 1 means 100% copper  $d$ , and the oxygen weight is simply 1 minus the copper weight).

becomes 78% at  $X$  and 56% at  $M$ . The two bottom bands have pure  $p$  character at the Brillouin zone center. The middle band achieves 43%  $d$  character at  $M$ , while the lower band has 21%  $d$  character at  $X$ . Note that the tight-binding Fermi surface, shown in the inset, has the qualitative shape expected in the cuprates from both the theory and experimental perspectives. However, its orbital content is only about 75%  $d$  on average, showing that the oxygen component is not negligible even if only one band crosses the Fermi level.

Note that  $\xi_{\mathbf{k}}$  can be written in terms of the  $3 \times 3$  Gell-Mann matrices [39]  $\lambda_i$  for cases  $i = 1$  to 8, while  $\lambda_0$  is the  $3 \times 3$  identity (see the Appendix for an explicit form of these matrices). This is useful in order to highlight the symmetry of its different terms:

$$\xi_{\mathbf{k}} = \frac{2}{3} \epsilon_p \lambda_0 + \frac{\sqrt{3}}{3} \epsilon_p \lambda_8 + 2t_{dp}(s_x \lambda_5 + s_y \lambda_7) - 4t_{pp}s_x s_y \lambda_1. \quad (18)$$

Since the  $\text{CuO}_2$  planes transform as  $D_{4h}$  and the Hamiltonian has to be invariant under the group operations, i.e., it has to transform as the  $A_{1g}$  representation of the group, we notice that in Eq. (18),  $\lambda_0$  and  $\lambda_8$  transform like  $A_{1g}$ , while  $\lambda_1$  transforms like  $B_{2g}$  and  $(\lambda_5, \lambda_7)$  transform like the two-dimensional representation  $E_g$  since they are combined with  $(s_x, s_y)$ , which transforms according to  $E_g$ .

The interacting term of the Hamiltonian can be written in terms of a pairing matrix  $P^{(0)}$  for the on-site same-oxygen case [Eq. (12)]:

$$P_{\mathbf{k}}^{(0)} = \begin{pmatrix} 2\Delta & 0 & 0 \\ 0 & -2\Delta & 0 \\ 0 & 0 & 0 \end{pmatrix}, \quad (19)$$

which can be written in terms of the  $\lambda_i$  matrices as

$$P_{\mathbf{k}}^{(0)} = 2\Delta\lambda_3. \quad (20)$$

For the extended pairing [Eq. (14)] the corresponding matrix  $P^{(pp)}$  is given by

$$P_{\mathbf{k}}^{(pp)} = \begin{pmatrix} 2\Delta \cos(k_x) & 0 & 0 \\ 0 & -2\Delta \cos(k_y) & 0 \\ 0 & 0 & 0 \end{pmatrix}, \quad (21)$$

which can be written in terms of the  $\lambda_i$  matrices as

$$P_{\mathbf{k}}^{(pp)} = 2\Delta \left[ \frac{[\cos(k_x) - \cos(k_y)]}{3} \lambda_0 + \frac{[\cos(k_x) + \cos(k_y)]}{2} \lambda_3 + \frac{\sqrt{3}[\cos(k_x) - \cos(k_y)]}{6} \lambda_8 \right]. \quad (22)$$

For the plaquette pairing operator [Eq. (15)] the corresponding matrix  $P^{(plaq)}$  is given by

$$P_{\mathbf{k}}^{(plaq)} = \begin{pmatrix} 2\Delta \cos(k_y) & 0 & 0 \\ 0 & -2\Delta \cos(k_x) & 0 \\ 0 & 0 & 0 \end{pmatrix}, \quad (23)$$

which can be written in terms of the  $\lambda_i$  matrices as

$$P_{\mathbf{k}}^{(plaq)} = 2\Delta \left[ \frac{[\cos(k_y) - \cos(k_x)]}{3} \lambda_0 + \frac{[\cos(k_y) + \cos(k_x)]}{2} \lambda_3 + \frac{\sqrt{3}[\cos(k_y) - \cos(k_x)]}{6} \lambda_8 \right]. \quad (24)$$

For the interorbital pairing operator  $\Delta_{Dpd}^\dagger$  the corresponding matrix  $P^{(pd)}$  [Eq. (13)] is given by

$$P_{\mathbf{k}}^{(pd)} = \begin{pmatrix} 0 & 0 & 2\Delta i s_x \\ 0 & 0 & -2\Delta i s_y \\ 2\Delta i s_x & -2\Delta i s_y & 0 \end{pmatrix}, \quad (25)$$

which can be written in terms of the  $\lambda_i$  matrices as

$$P_{\mathbf{k}}^{(pd)} = 2i\Delta(s_x\lambda_4 - s_y\lambda_6). \quad (26)$$

Thus, the effective interaction term can be constructed in terms of a spin-singlet pair operator that transforms according to the irreducible representation  $B_{1g}$  of  $D_{4h}$  [40]. In the case of  $P^{(0)}$  the symmetry of the pairing term is given by the matrix  $\lambda_3$ , which transforms according to  $B_{1g}$ . For  $P^{(pp)}$  in Eq. (22) note that the terms that contain  $\lambda_0$  and  $\lambda_8$ , which transform like  $A_{1g}$ , are multiplied by  $\cos(k_x) - \cos(k_y)$ , which transforms like  $B_{1g}$ , while the term that contains  $\lambda_3$ , which transforms like  $B_{1g}$ , is multiplied by  $\cos(k_x) + \cos(k_y)$ , which transforms like  $A_{1g}$ . A similar analysis for  $P^{(plaq)}$  in Eq. (24) shows that it also transforms like  $B_{1g}$ . The interorbital pairing operator also transforms as  $B_{1g}$  because it combines  $(s_x, s_y)$  with  $(\lambda_4, \lambda_6)$ , each transforming like  $E_g$ . Finally, for completeness, we present the pairing matrices for the traditional  $d$ -wave operator of the single- and three-orbital Hubbard models presented in Eqs. (4) and (5). For  $\Delta_D^\dagger$  the

corresponding matrix  $P^{(D)}$  is

$$P_{\mathbf{k}}^{(D)} = \begin{pmatrix} 0 & 0 & 0 \\ 0 & 0 & 0 \\ 0 & 0 & 2\Delta[\cos(k_x) - \cos(k_y)] \end{pmatrix}, \quad (27)$$

which can be written in terms of the  $\lambda_i$  matrices as

$$P_{\mathbf{k}}^{(D)} = 2\Delta[\cos(k_x) - \cos(k_y)](\lambda_0 - \sqrt{3}\lambda_8), \quad (28)$$

and for  $\Delta_{D3B}^\dagger$  the corresponding matrix  $P^{(D3B)}$  is

$$P_{\mathbf{k}}^{(D3B)} = 2\Delta[\cos(k_x) - \cos(k_y)] \begin{pmatrix} 1 & 0 & 0 \\ 0 & 1 & 0 \\ 0 & 0 & 1 \end{pmatrix}, \quad (29)$$

which can be written in terms of the  $\lambda_i$  matrices as

$$P_{\mathbf{k}}^{(D3B)} = 2\Delta[\cos(k_x) - \cos(k_y)]\lambda_0. \quad (30)$$

In summary, for the canonical widely used operators the  $B_{1g}$  symmetry is just directly given by the factor  $\cos(k_x) - \cos(k_y)$ , while for our operators deducing the  $d$ -wave character requires a careful analysis.

Another way of verifying the  $d$ -wave symmetry of the proposed pairing operators is the calculation of the band structure via the resulting  $6 \times 6$  Bogoliubov–de Gennes Hamiltonian given by

$$H_{\text{BdG}} = \sum_{\mathbf{k}} \Psi_{\mathbf{k}}^\dagger H_{\mathbf{k}}^{\text{MF}} \Psi_{\mathbf{k}}, \quad (31)$$

with the definitions

$$\Psi_{\mathbf{k}}^\dagger = (p_{\mathbf{k},x,\uparrow}^\dagger, p_{\mathbf{k},y,\uparrow}^\dagger, d_{\mathbf{k},\uparrow}^\dagger, p_{-\mathbf{k},x,\downarrow}, p_{-\mathbf{k},y,\downarrow}, d_{-\mathbf{k},\downarrow}) \quad (32)$$

and

$$H_{\mathbf{k}}^{\text{MF}} = \begin{pmatrix} (H_{\text{TB}}(\mathbf{k}) - \mu_e\lambda_0) & P^{(\alpha)}(\mathbf{k}) \\ (P^{(\alpha)})^\dagger(\mathbf{k}) & -(H_{\text{TB}}(\mathbf{k}) - \mu_e\lambda_0) \end{pmatrix}, \quad (33)$$

where the label  $\alpha$  takes the values  $0, pp, pd, plaq, D$ , or  $D3B$  and we have included the chemical potential  $\mu_e$  in the tight-binding term to ensure that the gap opens at the Fermi surface.

Diagonalizing the mean-field Hamiltonian, we find that a  $d$ -wave gap opens at the chemical potential. The resulting band structures for  $\alpha = 0$  and  $pp$  are shown in Fig. 5 for a  $100 \times 100$  lattice at a density of 4.9 electrons per unit cell (5 electrons per unit cell corresponds to the undoped case) along the main directions in momentum space for various values of  $\Delta$ . Results for  $\Delta = 0$  are shown to indicate the noninteracting Fermi surface. The results for the on-site pairing operator  $D_0$  ( $\alpha = 0$ ) are shown in Fig. 5(a), while those for the extended operator  $D_{pp}$  ( $\alpha = pp$ ) are in Fig. 5(b). In Figs. 5(c) and 5(d) it can be seen that for both  $\Delta = 0.3$  and  $0.5$  a gap opens at the antinodal position  $X$  but the node along the diagonal direction  $\Gamma$ - $M$  remains, indicating the  $d$ -wave symmetry of the gap, as expected [41]. In addition, note that the interaction distorts only the bands close to the Fermi surface, and we observe a very flat dispersion of the band that defines the gap at  $X$ , in agreement with recent experiments [16]. The results for the plaquette, interorbital, and traditional operators look very similar and are not shown explicitly.

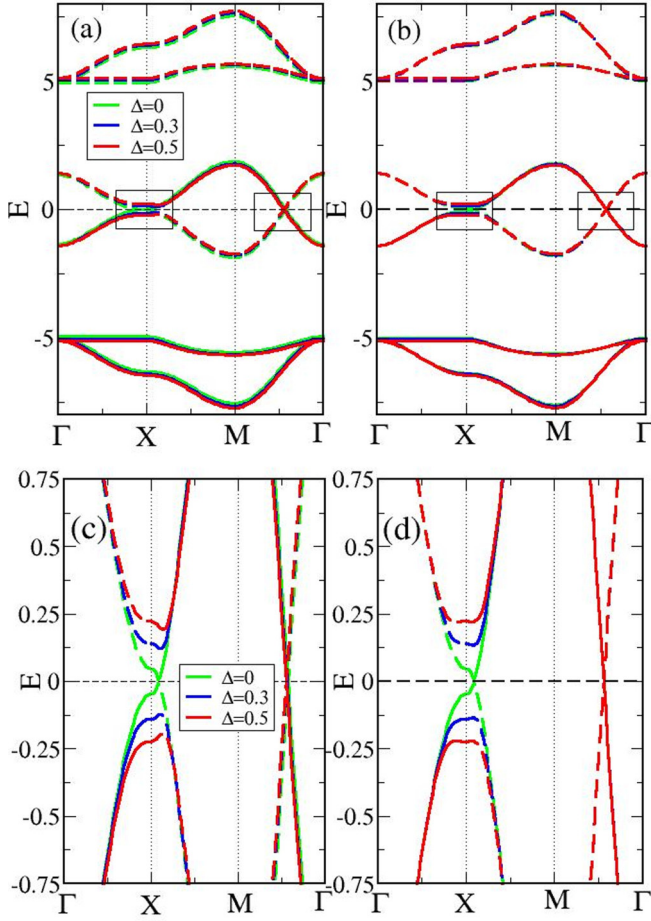


FIG. 5. Band dispersion for the mean-field Hamiltonians with  $B_{1g}$  pairing. (a) On-site  $D_0$  and (b) extended  $D_{pp}$  for the indicated values of the pairing order parameter  $\Delta$  at a density of 4.9 electrons per unit cell. (c) Detail of the areas inside rectangular boxes in (a); (d) detail of the areas inside rectangular boxes in (b). The dashed lines indicate ‘‘shadow’’ bands.

### B. Stability of the $d$ -wave state

The next aspect to explore is the stability of the pairing state with a finite gap. To study this issue we need to evaluate the energy of the mean-field Hamiltonian vs  $\Delta$  for different values of the pairing strength  $V$ , where  $\Delta = V \langle p_{-\mathbf{k},\mu,\downarrow} p_{\mathbf{k},\mu,\uparrow} \rangle$  for the on-site pairing  $D_0$ , which we assume is the same for all values of  $\mu$ . The total energy is

$$E = \sum_{\mathbf{k}} \left[ \sum_{i=1}^3 (\epsilon_i(\mathbf{k}) - \mu_e) - E_i(\mathbf{k}) \right] + \frac{\Delta^2 N}{V}, \quad (34)$$

where  $\epsilon_i(\mathbf{k})$  are the eigenvalues of the tight-binding term,  $E_i$  are the three negative eigenvalues of the mean-field matrix (where the chemical potential has been included), and  $N$  is the number of sites of the large but finite cluster used. The appropriate fermionic operators need to be used in the expression of  $\Delta$  for the remaining  $d$ -wave pairing operators.

We have observed that any finite value of  $V$  stabilizes the proposed pairing states, similar to what happens in the negative- $U$  Hubbard model. The small values of  $\Delta$  that minimize the energy for the different values of  $V$  are indicated with

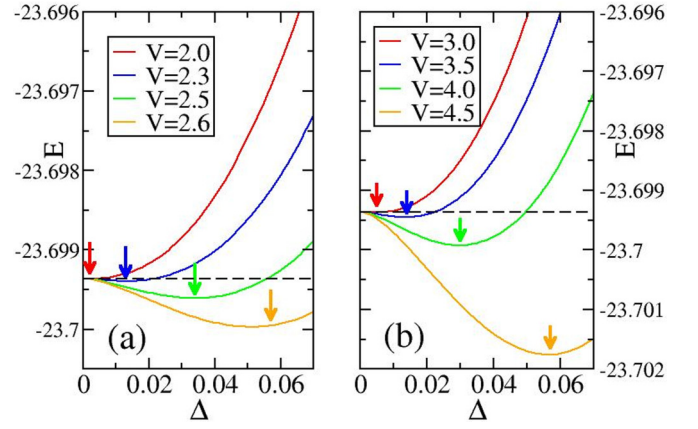


FIG. 6. Total energy versus  $\Delta$  at various values of  $V$  for (a) the on-site  $D_0$  and (b) the extended  $D_{pp}$  pairing operators. Arrows indicate the minima in the energies.  $\Delta$  and  $E$  are in units of eV.

an arrow in Figs. 6(a) and 6(b) for the pairing operators  $D_0$  and  $D_{pp}$ . Experimentally, the value of the superconducting gap in the cuprates ranges from 20 to 40 meV [42]. Since the gap in our model is equal to  $2\Delta$ , we see from Fig. 6 that  $V \sim 2.4$  ( $V \sim 3.6$ ) provides a reasonable value of  $\Delta$  for the minimum energy for on-site (extended) pairing. While all the  $d$ -wave pairing operators open a gap in the density of states as soon as  $V$  is finite, we observed that all the pairing states that include  $d$  orbitals produce larger gaps than the pure  $p$ -orbital operators at a fixed value of the attraction  $V$ . This becomes clear as we obtain the value of  $V$  needed in each case to open a gap similar to the one observed in the cuprates. In Table I we present the values of the attraction that stabilizes a gap of 20 meV in each case, and it can be seen that  $V < 1$  eV ( $V > 1$  eV) is needed for operators that (do not) involve  $d$  orbitals.

Thus, the mean-field results appear to indicate that pairing operators that involve the  $d$  orbital need a much smaller attraction to produce a superconducting gap similar to the one observed in the cuprates. This is probably due to the fact that in the mean-field calculations the gap opens around the noninteracting Fermi surface, which, as shown in Fig. 4, is mostly a  $d$  band. In the cuprates, however, it is expected that the band that forms the noninteracting Fermi surface would generate upper and lower bands due to the Coulomb repulsion at the Cu, and the Fermi surface upon doping will occur in a  $p$ - $d$  hybridized band [43], identified as a Zhang-Rice band in photoemission [24,44–46]. Due to the higher weight of the  $p$  orbitals in this band, it is expected that the  $p$ -based compact

TABLE I.  $V_{\Delta=20 \text{ meV}}$  indicates the value of the attraction that produces a total gap of 40 meV for the corresponding  $d$ -wave pairing.

Operator label	$V_{\Delta=20 \text{ meV}}$ (eV)
$D_0$	2.38
$D_{pp}$	3.68
$D_{plaq}$	3.50
$D_{pd}$	0.50
$D_D$	0.13
$D_{D3B}$	0.15

$d$ -wave order parameters proposed here may work better than the traditionally used pairing operators [47].

## VI. PHENOMENOLOGICAL MODEL

Finally, if we replace  $\Delta$  by  $2V\gamma_\nu p_{\mathbf{j}+\hat{\nu}/2, \nu, \downarrow} p_{\mathbf{j}+\hat{\nu}/2, \nu, \uparrow}$  instead of the average value of the pairing operator in Eq. (12), we obtain a phenomenological interaction that should promote the on-site  $d$ -wave pairing  $D_0$  given by

$$\begin{aligned} H_{\text{int}} &= -4V \sum_{\mathbf{j}, \mu, \nu} \gamma_\mu \gamma_\nu p_{\mathbf{j}+\hat{\mu}/2, \mu, \uparrow}^\dagger p_{\mathbf{j}+\hat{\mu}/2, \mu, \downarrow}^\dagger p_{\mathbf{j}+\hat{\nu}/2, \nu, \downarrow} p_{\mathbf{j}+\hat{\nu}/2, \nu, \uparrow} \\ &= -4V \sum_{\mathbf{j}, \mu} n_{\mathbf{j}+\hat{\mu}/2, \mu, \uparrow} n_{\mathbf{j}+\hat{\mu}/2, \mu, \downarrow} \\ &\quad + 4V \sum_{\mathbf{j}, \mu \neq \nu} p_{\mathbf{j}+\hat{\mu}/2, \mu, \uparrow}^\dagger p_{\mathbf{j}+\hat{\nu}/2, \nu, \downarrow} p_{\mathbf{j}+\hat{\mu}/2, \mu, \downarrow}^\dagger p_{\mathbf{j}+\hat{\nu}/2, \nu, \uparrow}. \end{aligned} \quad (35)$$

The first term is an effective on-site attraction in the O sites, while the second term involves the four O atoms that surround the Cu at site  $\mathbf{j}$  and is repulsive. While it is unlikely that terms of this form could be dynamically generated by the long-range Coulomb repulsion and a short-range attraction induced by antiferromagnetic fluctuations, it is important to remember that the electron-phonon interaction in BCS superconductors does not lead to the instantaneous on-site attraction of the negative- $U$  Hubbard model. However, this model has been an important phenomenological tool to study the behavior of  $s$ -wave superconductors, both with weak and strong attraction. In fact, numerical studies of the negative  $U$  Hubbard model show that in the weak-coupling regime in which the Cooper pairs are very extended in real space, the extended  $s$ -wave pairing operator is more enhanced than the on-site operator, despite the fact that both develop long-range order. This behavior is reversed in the strong-coupling limit in which the pairs are localized, and thus, the on-site pairing operator prevails [48]. Thus, it is possible that the Hamiltonian here proposed could play a similar role but for  $d$ -wave superconductors. In order to observe long-range order with this very local pairing operator it may be necessary to use a very large value of  $V$  to allow for a higher  $p$ - $d$  hybridization at the Fermi surface. In addition, we want to point out that the negative- $U$  Hubbard model has been simulated using optical lattices, but it has been very challenging to do the same for the repulsive case, and thus, the observation of  $d$ -wave superconductivity in these lattices has been elusive [49]. Simulating the present phenomenological model, with an explicit attraction, via optical lattices may offer an alternative avenue towards this goal.

## VII. CONCLUSIONS

Summarizing, in this effort intracell  $\text{CuO}_2$ , three intraorbital and one interorbital, pairing operators with  $d$ -wave

symmetry have been proposed for the high-critical-temperature cuprates. These operators are more local (more compact in size) than those previously employed in numerical studies, and thus, they may produce a stronger signal when their long-range behavior in finite systems is studied with numerical many-body techniques. These operators can be used in models for the  $\text{CuO}_2$  planes that include longer-range hoppings or additional orbitals [50]. In addition, they may be able to account for the small size of the pairs recently experimentally observed in the cuprates via angle-resolved photoemission methods. At the mean-field level, the flatness of the band that forms the gap at the antinodes is reproduced, and it is demonstrated that the size of the superconducting gap experimentally observed is obtained even with a moderate attraction [51]. The next step would be to evaluate more properties of these pairing operators at the mean-field level and, even more importantly, to calculate their pairing correlations in the three-orbital Hubbard model employing unbiased computational techniques.

## ACKNOWLEDGMENTS

The authors were supported by the U.S. Department of Energy (DOE), Office of Science, Basic Energy Sciences (BES), Materials Sciences and Engineering Division.

## APPENDIX: $\lambda_i$ MATRICES

The  $\lambda_i$  matrices used in the text are presented here:

$$\lambda_0 = \begin{pmatrix} 1 & 0 & 0 \\ 0 & 1 & 0 \\ 0 & 0 & 1 \end{pmatrix}, \quad \lambda_1 = \begin{pmatrix} 0 & 1 & 0 \\ 1 & 0 & 0 \\ 0 & 0 & 0 \end{pmatrix},$$

$$\lambda_2 = \begin{pmatrix} 0 & -i & 0 \\ i & 0 & 0 \\ 0 & 0 & 0 \end{pmatrix}, \quad \lambda_3 = \begin{pmatrix} 1 & 0 & 0 \\ 0 & -1 & 0 \\ 0 & 0 & 0 \end{pmatrix},$$

$$\lambda_4 = \begin{pmatrix} 0 & 0 & 1 \\ 0 & 0 & 0 \\ 1 & 0 & 0 \end{pmatrix}, \quad \lambda_5 = \begin{pmatrix} 0 & 0 & -i \\ 0 & 0 & 0 \\ i & 0 & 0 \end{pmatrix},$$

$$\lambda_6 = \begin{pmatrix} 0 & 0 & 0 \\ 0 & 0 & 1 \\ 0 & 1 & 0 \end{pmatrix}, \quad \lambda_7 = \begin{pmatrix} 0 & 0 & 0 \\ 0 & 0 & -i \\ 0 & i & 0 \end{pmatrix},$$

$$\lambda_8 = \frac{1}{\sqrt{3}} \begin{pmatrix} 1 & 0 & 0 \\ 0 & 1 & 0 \\ 0 & 0 & -2 \end{pmatrix}.$$

[1] C. C. Tsuei, J. R. Kirtley, C. C. Chi, L. S. Yu-Jahnes, A. Gupta, T. Shaw, J. Z. Sun, and M. B. Ketchen, *Phys. Rev. Lett.* **73**, 593 (1994).

[2] J. R. Kirtley, C. C. Tsuei, J. Z. Sun, C. C. Chi, L. S. Yu-Jahnes, A. Gupta, M. Rupp, and M. B. Ketchen, *Nature (London)* **373**, 225 (1995).



- [3] R. T. Scalettar, E. Y. Loh, J. E. Gubernatis, A. Moreo, S. R. White, D. J. Scalapino, R. L. Sugar, and E. Dagotto, *Phys. Rev. Lett.* **62**, 1407 (1989).
- [4] A. Moreo and D. J. Scalapino, *Phys. Rev. Lett.* **66**, 946 (1991).
- [5] M. Randeria, N. Trivedi, A. Moreo, and R. T. Scalettar, *Phys. Rev. Lett.* **69**, 2001 (1992).
- [6] E. Dagotto, J. Riera, Y. C. Chen, A. Moreo, A. Nazarenko, F. Alcaraz, and F. Ortolani, *Phys. Rev. B* **49**, 3548 (1994).
- [7] A. Nazarenko, A. Moreo, E. Dagotto, and J. Riera, *Phys. Rev. B* **54**, R768 (1996).
- [8] D. S. Rokhsar and S. A. Kivelson, *Phys. Rev. Lett.* **61**, 2376 (1988).
- [9] F. F. Assaad, M. Imada, and D. J. Scalapino, *Phys. Rev. Lett.* **77**, 4592 (1996).
- [10] Phenomenologically, the coupling of fermions with classical pairing fields leads to  $d$ -wave pairing [see M. Mayr, G. Alvarez, C. Sen, and E. Dagotto, *Phys. Rev. Lett.* **94**, 217001 (2005)], but we are searching for purely fermionic systems.
- [11] D. C. Johnston, *Adv. Phys.* **59**, 803 (2010).
- [12] P. Dai, J. P. Hu, and E. Dagotto, *Nat. Phys.* **8**, 709 (2012).
- [13] Y. Wan and Q.-H. Wang, *Europhys. Lett.* **85**, 57007 (2009).
- [14] M. Daghofer, A. Moreo, J. A. Riera, E. Arrigoni, D. J. Scalapino, and E. Dagotto, *Phys. Rev. Lett.* **101**, 237004 (2008).
- [15] C. B. Bishop, G. Liu, E. Dagotto, and A. Moreo, *Phys. Rev. B* **93**, 224519 (2016).
- [16] H. Li, X. Zhou, S. Parham, K. N. Gordon, R. D. Zhong, J. Schneeloch, G. D. Gu, Y. Huang, H. Berger, G. B. Arnold, and D. S. Dessau, [arXiv:1809.02194](https://arxiv.org/abs/1809.02194).
- [17] M. S. D. A. Hussein, E. Dagotto, and A. Moreo, *Phys. Rev. B* **99**, 115108 (2019).
- [18] E. Arrigoni, M. Aichhorn, M. Daghofer, and W. Hanke, *New J. Phys.* **11**, 055066 (2009).
- [19] E. W. Huang, C. B. Mendl, S. Liu, S. Johnston, H.-C. Jiang, B. Moritz, and T. P. Devereaux, *Science* **358**, 1161 (2017).
- [20] E. Dagotto and J. R. Schrieffer, *Phys. Rev. B* **43**, 8705(R) (1991).
- [21] V. J. Emery and G. Reiter, *Phys. Rev. B* **38**, 11938(R) (1988).
- [22] M. S. Hybertsen, M. Schlüter, and N. E. Christensen, *Phys. Rev. B* **39**, 9028 (1989).
- [23] M. S. D. A. Hussein, M. Daghofer, E. Dagotto, and A. Moreo, *Phys. Rev. B* **98**, 035124 (2018).
- [24] Z.-X. Shen, J. W. Allen, J. J. Yeh, J.-S. Kang, W. Ellis, W. Spicer, I. Lindau, M. B. Maple, Y. D. Dalichaouch, M. S. Torikachvili, J. Z. Sun, and T. H. Geballe, *Phys. Rev. B* **36**, 8414 (1987).
- [25] J. W. Allen, C. G. Olson, M. B. Maple, J.-S. Kang, L. Z. Liu, J.-H. Park, R. O. Anderson, W. P. Ellis, J. T. Markert, Y. Dalichaouch, and R. Liu, *Phys. Rev. Lett.* **64**, 595 (1990).
- [26] B. O. Wells, Z.-X. Shen, A. Matsuura, D. M. King, M. A. Kastner, M. Greven, and R. J. Birgeneau, *Phys. Rev. Lett.* **74**, 964 (1995).
- [27] A. Damascelli, Z. Hussain, and Z.-X. Shen, *Rev. Mod. Phys.* **75**, 473 (2003).
- [28] F. C. Zhang and T. M. Rice, *Phys. Rev. B* **37**, 3759 (1988).
- [29] E. Dagotto, *Rev. Mod. Phys.* **66**, 763 (1994).
- [30] D. J. Scalapino, *Phys. Rep.* **250**, 329 (1995).
- [31] G. Dopf, A. Muramatsu, and W. Hanke, *Phys. Rev. B* **41**, 9264 (1990).
- [32] Z. B. Huang, H. Q. Lin, and J. E. Gubernatis, *Phys. Rev. B* **63**, 115112 (2001).
- [33] P. B. Littlewood, C. M. Varma, and E. Abrahams, *Phys. Rev. Lett.* **63**, 2602 (1989).
- [34] C. D. Batista and A. A. Aligia, *Phys. Rev. B* **48**, 4212(R) (1993).
- [35] S. Zhang, *Phys. Rev. B* **42**, 1012(R) (1990).
- [36] W.-L. You, S.-J. Gu, G.-S. Tian, and H.-Q. Lin, *Phys. Rev. B* **79**, 014508 (2009).
- [37] The explicit form of the commutator is given by  $[H_{pd}, \Delta_{Dpd}^\dagger] = -t_{pd} \Delta_{Dpp}^\dagger - t_{pd} \Delta_D^\dagger$ .
- [38] The explicit form of the operator is given by  $\Delta_{Dpd2}^\dagger(\mathbf{j}) = \sum_{\mu, \nu \neq \mu, \sigma} f_\sigma \gamma_\nu d_{\mathbf{j}, \sigma}^\dagger P_{\mathbf{j}+\nu+\hat{\mu}/2, \mu, -\sigma}^\dagger$ , where  $\mu = \pm x, \pm y$  and  $\nu = \pm x, \pm y$ , with  $\nu = \pm x$  if  $\mu = \pm y$  and vice versa.
- [39] L. Schiff, *Quantum Mechanics*, 3rd ed. (McGraw-Hill, Tokyo, 1968).
- [40] M. Daghofer, A. Nicholson, A. Moreo, and E. Dagotto, *Phys. Rev. B* **81**, 014511 (2010).
- [41] We have checked numerically that the nodes along  $\Gamma$ - $M$  remain, even at very strong pairing interactions. This is due to the  $d$ -wave symmetry of the operators. While we could not obtain an analytical expression for the eigenvalues of the mean-field matrices, we expect that the contribution proportional to  $\Delta$ , the pairing strength, should contain linear combinations that vanish when  $k_x = k_y$  to satisfy the  $B_{1g}$  symmetry of the pairing operators.
- [42] T. Yoshida, M. Hashimoto, I. M. Vishik, Z.-X. Shen, and A. Fujimori, *J. Phys. Soc. Jpn.* **81**, 011006 (2012).
- [43] J. G. Zaanen, G. A. Sawatzky, and J. W. Allen, *Phys. Rev. Lett.* **55**, 418 (1985).
- [44] Y. Sakurai, M. Itou, B. Barbiellini, P. E. Mijnders, R. S. Markiewicz, S. Kaprzyk, J.-M. Gillet, S. Wakimoto, M. Fujita, S. Basak, Y. J. Wang, W. Al-Sawai, H. Lin, A. Bansil, and K. Yamada, *Science* **332**, 698 (2011).
- [45] C. T. Chen, F. Sette, Y. Ma, M. S. Hybertsen, E. B. Stechel, W. M. C. Foulkes, M. Schluter, S. W. Cheong, A. S. Cooper, L. W. Rupp, B. Batlogg, Y. L. Soo, Z. H. Ming, A. Krol, and Y. H. Kao, *Phys. Rev. Lett.* **66**, 104 (1991).
- [46] E. Pellegrin, N. Nücker, J. Fink, S. L. Molodtsov, A. Gutiérrez, E. Navas, O. Strelbel, Z. Hu, M. Domke, G. Kaindl, S. Uchida, Y. Nakamura, J. Markl, M. Klauda, G. Saemann-Ischenko, A. Krol, J. L. Peng, Z. Y. Li, and R. L. Greene, *Phys. Rev. B* **47**, 3354 (1993).
- [47] Calculations including a mean-field treatment of the Coulomb repulsion on the Cu electrons are in progress and will be presented in a future publication.
- [48] M. Guerrero, G. Ortiz, and J. E. Gubernatis, *Phys. Rev. B* **62**, 600 (2000).
- [49] W. Hofstetter and T. Qin, *J. Phys. B* **51**, 082001 (2018).
- [50] L. F. Feiner, J. H. Jefferson, and R. Raimondi, *Phys. Rev. Lett.* **76**, 4939 (1996).
- [51] While in BCS superconductors an infinitesimal attraction stabilizes the superconducting state, this may not be the case in the cuprates, and in addition, when the Coulomb interaction is taken into account, the orbital content at the chemical potential for a doped system will contain more  $p$  contributions than in the noninteracting case.